Vol. 610: 1–13, 2019
https://doi.org/10.3354/meps12839

MARINE ECOLOGY PROGRESS SERIES
Mar Ecol Prog Ser

Published February 1

FEATURE ARTICLE

Broader foraging range of ancient short-tailed albatross populations into California coastal waters based on bulk tissue and amino acid isotope analysis

Natasha L. Vokhshoori[1,2,*], Matthew D. McCarthy[1], Paul W. Collins[3], Michael A. Etnier[4], Torben Rick[5], Masaki Eda[6], Jessie Beck[7], Seth D. Newsome[2]

[1]Ocean Sciences Department, University of California, Santa Cruz, Santa Cruz, California 95060, USA
[2]Biology Department, University of New Mexico, Albuquerque, New Mexico 87131, USA
[3]Santa Barbara Museum of Natural History, Santa Barbara, California 93105, USA
[4]Anthropology Department, Western Washington University, Bellingham, Washington 98225, USA
[5]Anthropology Department, Smithsonian Institution, Washington, DC 20560, USA
[6]Hokkaido University Museum, Hokkaido University, Sapporo 004-0006, Japan
[7]Oikonos Ecosystem Knowledge, Santa Cruz, California 95060, USA

ABSTRACT: The short-tailed albatross *Phoebastria albatrus* was nearly driven to extinction in the early 20th century, but is one of the most common seabirds found in coastal archaeological sites in Japan, the Aleutian Islands, and the Channel Islands off southern California. Today, this species nests on only 2 islands off southern Japan and spends the majority of its time foraging in waters west of the Aleutians. We used carbon and nitrogen isotope analysis of bulk tissue (bone collagen) and its constituent amino acids from modern samples of all 3 North Pacific albatross species as well as ancient short-tailed albatross to show that ancient short-tailed albatross foraged east of the Aleutian Islands more frequently than their modern counterparts. Isotope mixing models correctly assigned each species to its known foraging habitats, validating our approach on ancient short-tailed albatross. Mixing models also showed that ancient short-tailed albatross from both western and eastern North Pacific archaeological sites spent more time in the California Current than their modern congeners. However, ancient albatross remains from archaeological sites off southern California are isotopically distinct from those found in sites from the western North Pacific, suggesting this species previously had a more complex population structure. We found that modern short-tailed albatross occupy a higher trophic level than their ancient counterparts, which may be due to their consumption of bait and offal from longline fisheries. As extant short-tailed albatross recover from historical overexploitation, the reconstruction of their historical ecology helps in identifying likely areas for foraging and possible breeding range expansion.

*Corresponding author: nvokhsho@ucsc.edu

Short-tailed albatross *Phoebastria albatrus* nesting on an egg at the main colony on Torishima, Tsubame-zaki, Japan.

Photo: Robert Suryan

KEY WORDS: Historical ecology · North Pacific albatrosses · Amino acid isotope analysis

1. INTRODUCTION

Studying the past ecology of extant but threatened marine species that have been subjected to direct (e.g. overfishing, pollution) and indirect (e.g. climate change) threats can provide a framework for conservation efforts by defining the ecological plasticity of species over evolutionarily relevant timescales (Swetnam et al. 1999, Jackson et al. 2001). Museum collec-

Publisher: Inter-Research · www.int-res.com

tions and archaeological sites contain materials that have been used to reconstruct ecological systems prior to extensive human disturbance (Olson & Hearty 2003, Newsome et al. 2007, Eda et al. 2012, Wiley et al. 2013). Such historical baselines offer insights into pre-exploitation conditions that can be important when designing management plans for species that currently occur in relict populations (Lotze & Worm 2009).

The short-tailed albatross *Phoebastria albatrus* is an example of a species that was driven to near extinction by human exploitation. Pre-exploitation population size has been estimated to be >1 million individuals distributed across ~14 colonies, but plummeted to ~100 individuals on 2 nesting colonies (Senkaku and Torishima Islands) off southern Japan before cessation of commercial harvest in 1933 (Hasegawa & DeGange 1982, USFWS 2008). Landmark conservation policies protecting albatross breeding colonies in the early 20th century (USFWS 2008) were followed by the emergence of another threat, industrialized fishing, which increased mortality from bycatch (Arata et al. 2009). Due to protection of colonies on land and adults at sea, along with successful translocation efforts, the current population is growing at carrying capacity and population size has reached several thousand individuals (Deguchi et al. 2017), though it remains well under historic estimates.

The Holocene coastal archaeological record (~11 200–300 yr BP) suggests that short-tailed albatross ranged from the mainland coast in the Japan and Okhotsk Seas, north to the Bering Strait and Aleutian Islands, and in the eastern Pacific from the Gulf of Alaska to Baja California (Yesner 1976, Hasegawa & DeGange 1982, Porcasi 1999, Eda & Higuchi 2004). Notably, short-tailed albatross are the dominant seabird species found in some central and southern California archaeological sites, particularly the Channel Islands (Porcasi 1999, Erlandson et al. 2011), which contrasts with their modern distribution that is primarily constrained to the western Pacific and Aleutian Islands (Suryan et al. 2006, Kuletz et al. 2014). This suggests that ancient populations spent more time foraging in the California Current than the current population, and perhaps also bred on islands in the eastern Pacific (Porcasi 1999).

Carbon ($\delta^{13}C$) and nitrogen ($\delta^{15}N$) isotope analysis of tissues archived in museum collections and archaeological sites is a powerful tool for studying past life histories of marine organisms (e.g. Burton et al. 2001, Newsome et al. 2007, Wiley et al. 2013). Isotope values of mobile marine consumers reflect a combination of the isotopic composition of the base of the food webs in which they forage, as well as diet composition. Consumers typically have higher isotope values than their food due to physiologically mediated isotopic discrimination that occurs during resource assimilation and tissue synthesis; such offsets are often called trophic discrimination factors (TDFs), and vary from 0 to 3 and 2 to 5‰ for $\delta^{13}C$ and $\delta^{15}N$ respectively (Vanderklift & Ponsard 2003, DeNiro & Epstein 1978). To untangle the sometimes confounding effects of diet composition from spatial variation in the (baseline) isotopic composition of primary producers, researchers have used compound-specific isotope analysis (CSIA) of $\delta^{13}C$ ($\delta^{13}C_{AA}$) and $\delta^{15}N$ ($\delta^{15}N_{AA}$) values of individual amino acids (AAs). Animals must acquire essential amino acids (EAAs) directly from their diet to build and maintain proteinaceous tissues, thus the $\delta^{13}C$ value of this class of AAs shows little to no isotopic fractionation as these molecules move up the food chain (Howland et al. 2003, McMahon et al. 2015). For $\delta^{15}N_{AA}$, certain AAs undergo significant isotopic discrimination during transamination and deamination linked to the central glutamate pool (McMahon & McCarthy 2016, O'Connell 2017), and as such are commonly termed trophic AAs (e.g. glutamic acid, proline). Other AAs (e.g. phenylalanine) show little nitrogen isotope discrimination with trophic level and are termed source AAs (McClelland & Montoya 2002, Popp et al. 2007, Chikaraishi et al. 2009). Thus, AA isotope analysis of tissues collected from mobile marine consumers has the capacity to simultaneously estimate trophic level (TL) and identify foraging habitat(s) that have distinct baseline isotope values (McMahon & McCarthy 2016).

Establishing the isotope signatures at the base of the food web of a given region is a prerequisite to tracing movement patterns of organisms with isotope analysis (Graham et al. 2010). Ocean circulation patterns and latitudinal gradients in abiotic factors such as temperature result in zones with distinct biogeochemical cycling, which drive the spatial distributions of isotope values (isoscapes) of primary producers and primary consumers at the base of marine food webs (Graham et al. 2010, McMahon et al. 2013, Vokhshoori et al. 2014, Vokhshoori & McCarthy 2014). For $\delta^{15}N$, spatial gradients in isotopic baselines are typically driven by relative rates of N-fixation versus denitrification, coupled with the extent of vertical mixing that supplies nitrate from intermediate water depths (Sigman et al. 2009). Baseline $\delta^{13}C$ gradients in marine systems are generally driven by a more complex mixture of biological and physicochemical controls, including sea surface temperature

and the concentration of dissolved CO_2 (Rau et al. 1989), phytoplankton physiology (Fry & Wainright 1991, Popp et al. 1998), growth rate (Laws et al. 1995), and the composition of the primary producer community (e.g. micro- versus macroalgae) (Larsen et al. 2013). These baseline isotope gradients have been used to study the movement of tuna (Madigan et al. 2014, Lorrain et al. 2015), sharks (Carlisle et al. 2012), sea turtles (Turner Tomaszewicz et al. 2017), and pinnipeds (Burton et al. 2001, Aurioles et al. 2006) in the North Pacific.

In this study, we first built a basin-scale $\delta^{13}C$ and $\delta^{15}N$ isoscape of the North Pacific, and then used archived tissues from museum collections and archaeological sites to reconstruct long-term temporal changes in the distribution patterns of short-tailed albatross. Our main objective was to use $\delta^{13}C$ and $\delta^{15}N$ analysis of both bulk tissue (bone collagen) and its constituent AAs to compare the foraging distribution and TL of ancient populations of short-tailed albatross relative to their modern counterparts and the other 2 albatross species endemic to the North Pacific: black-footed *P. nigripes* and Laysan *P. immutabilis*. We compared the modern isotope data set to satellite tracking data as a means to validate our approach. Ancient short-tailed albatross samples were sourced from 4 geographically distinct regions in the western and eastern North Pacific, while modern samples were largely sourced from bycatch programs in the central and eastern North Pacific. We used published data of primary producers and primary consumers to build an isoscape of the North Pacific to interpret our bulk tissue and AA isotope patterns from albatrosses, and test the hypothesis that ancient populations of short-tailed albatross spent a substantial portion of their annual life cycle foraging in the productive California Current in the eastern Pacific, in contrast to their modern counterparts. This new information on the past ecology of short-tailed albatross provides general predictions as to where this species may expand their range as it recovers from historical over-exploitation.

2. MATERIALS AND METHODS

2.1. Sample collection and preparation

Modern Laysan, black-footed, and short-tailed albatross bone elements were collected from US bycatch necropsy programs. Ancient short-tailed albatross bone fragments were curated at either the Santa Barbara Natural History Museum, Burke Museum of Natural History, National Museum of Natural History, Oregon Museum of Natural and Cultural History, or the Hokkaido University Museum (see Supplement 1 at www.int-res.com/articles/suppl/m610p001_supp1–6.pdf; this URL applies to Supplements 1 to 6). To extract collagen from bone, a ~25 mg bone fragment of each sample was demineralized in 0.5 N hydrochloric acid (HCl) for ~24 h at ~5°C. Each sample was then rinsed to neutrality 3 times with deionized water, lipid-extracted by soaking in a solvent solution of 2:1 chloroform/methanol for ~72 h (solvent solution replaced every ~24 h), and finally lyophilized for 24 h.

2.2. Bulk and amino acid $\delta^{13}C$ and $\delta^{15}N$ analysis

A total of 0.5 mg of collagen was weighed into 3 × 5 mm tin capsules, and carbon ($\delta^{13}C$) and nitrogen ($\delta^{15}N$) isotope values were measured on a Costech (4010) elemental analyzer coupled to a Thermo Scientific Delta V Plus isotope ratio mass spectrometer (IRMS) at the University of New Mexico Center for Stable Isotopes (UNM-CSI). Within-run analytical error was assessed via repeated analysis of internal proteinaceous reference materials (Pugel and Acentailide) and was estimated to be ±0.2‰ for both $\delta^{13}C$ and $\delta^{15}N$. Isotopes values are reported using delta (δ) notation in parts per thousand (‰): $\delta^{13}C$ or $\delta^{15}N = [(R_{sample} / R_{standard}) - 1] \times 1000$, where R is the ratio of heavy to light isotope of the sample (R_{sample}) and standard ($R_{standard}$), respectively, referenced to atmospheric N_2 (air) for $\delta^{15}N$ and Vienna PeeDee Belemnite (PDB) for $\delta^{13}C$. Ancient seabird bones (>1000 yr) were corrected for the Suess Effect; the corrections considered a rate of $\delta^{13}C$ decrease in the atmosphere of 0.16‰ decade^{-1} since 1960, and of 0.05‰ decade^{-1} between 1860 and 1960 (Francey et al. 1999, Quay et al. 1992).

Total $\delta^{13}C_{AA}$ and $\delta^{15}N_{AA}$ values were measured as trifluoroacetyl isopropyl ester (TFA-IP) derivatives after acid hydrolysis. First, bone collagen samples were hydrolyzed by adding ~6–8 mg collagen into 1 ml of 6 N HCl at 110°C for 20 h; tubes were flushed with N_2 before being capped to remove oxygen. After drying at 60°C under N_2, AA isopropyl esters were prepared with a 1:4 mixture of acetyl chloride: isopropanol at 110°C for 60 min and then aceytlated using a 1:1 mixture of dichloromethane (DCM) and trifluoroacetic anhydride (TFAA) at 110°C for 10 min (Silfer et al. 1991). Samples were dried and redissolved in DCM for AA analysis. The $\delta^{13}C_{AA}$ and $\delta^{15}N_{AA}$ values were measured using a TRACE 1310 gas chromatograph with IsoLink 2 combustion unit coupled to a Thermo Scientific Delta V Plus IRMS at

UNM-CSI, or a Varian gas chromatograph coupled to a Finnegan Delta-Plus IRMS at the University of California Santa Cruz Stable Isotope Laboratory. AA stock standard and a cyanobacteria sample were analyzed on both instruments for inter-laboratory comparison and performance of instruments (Supplement 2).

Using this method, we measured $\delta^{13}C$ and $\delta^{15}N$ values of the following AAs in bone collagen: alanine (Ala), glycine (Gly), threonine (Thr), serine (Ser), valine (Val), leucine (Leu), isoleucine (Ile), proline (Pro), aspartic acid (Asp), glutamic acid (Glu), phenylalanine (Phe), tyrosine (Tyr), and lysine (Lys). All samples were analyzed in duplicate for carbon and triplicate for nitrogen. Measured $\delta^{13}C_{AA}$ values were corrected for the carbon added during derivatization following the approach of Silfer et al. (1991) and Hare et al. (1991). Reproducibility as estimated with standard deviation for collagen samples was typically less than <0.3‰ (range: 0.0–0.6‰) for carbon and <0.5‰ for nitrogen (range: 0.1–1.3 ‰).

2.3. Data analysis

We tested several working CSIA-based trophic level equations; however, we chose the $TDF_{Pro\text{-}Phe}$ derived from McMahon & McCarthy (2016):

$$TL_{Proline} = 1 + [(\delta^{15}N_{Pro} - \delta^{15}N_{Phe}) - 3.1] / 5.2 \quad (1)$$

where 3.1‰ is the typical TDF of plankton and other lower TL marine organisms (e.g. Chikaraishi et al. 2009, 2014) and 5.2‰ is the $TDF_{Pro\text{-}Phe}$ from a meta-analysis of controlled feeding studies (McMahon & McCarthy 2016) and a mean propagated error of 0.2; see Supplement 3 for a more detailed description of why we chose to use $TDF_{Pro\text{-}Phe}$ to estimate TL.

Two approaches were used to estimate baseline isotope values based on CSIA. The first used the non-fractionating $\delta^{15}N_{AA}$ source ($\delta^{15}N_{Baseline}$) and $\delta^{13}C_{AA}$ essential amino acids ($\delta^{13}C_{Baseline}$):

$$\delta^{15}N_{Baseline} = \delta^{15}N_{Phe} - 0.4(TL) \quad (2)$$

where $\delta^{15}N_{Phe}$ is the isotope value of an albatross minus a small enrichment factor (0.4‰) due to trophic transfer (Chikaraishi et al. 2009), and

$$\delta^{13}C_{Baseline} = 1.1 \times (\delta^{13}C_{Phe}) + 7.4 \quad (3)$$

where $\delta^{13}C_{Phe}$ is the measurement EAA isotope value, 1.1 is the slope of a line between measured $\delta^{13}C$ bulk and $\delta^{13}C_{Phe}$ values from phytoplankton and 7.4 is the associated *y*-intercept (Supplement 4).

The second approach used bulk tissue isotope values corrected for mean TL estimated using Eq. (1) and applied to the bulk isotope value of each individual from that group. We used this record for the isotope mixing model because it is a much larger data set, and therefore enhances statistical resolution:

$$\delta^{13}C_{TDF\text{-}CORR} = \delta^{13}C_{Bulk} - [1.5 + (1.1 \times \text{mean } TL_{Pro})] \quad (4)$$

and

$$\delta^{15}N_{TDF\text{-}CORR} = \delta^{15}N_{Bulk} - (3.1 \times \text{mean } TL_{Pro}) \quad (5)$$

where 1.5‰ is the $\delta^{13}C$ offset between bone collagen of a piscivorous seabird and diet ($\delta^{15}N$ showed virtually no offset), and 1.1 and 3.1‰ are the TDFs for $\delta^{13}C$ and $\delta^{15}N$ respectively (Hobson & Clark 1992).

For analysis, *t*-tests, ANOVAs and mixing models were performed in R (v.3.3.1) with RStudio interface (v.0.98.1028). Normality (Q-Q plots) and homoscedasticity (Bartlett's test) of the data were verified before statistical analyses. We calculated standard ellipse areas (SEA) for each albatross population using the stable isotope Bayesian ellipses in R package (SIBER; Jackson et al. 2011) and used the stable isotope analysis in R package (SIAR; Parnell et al. 2010) to run mixing models.

3. RESULTS

3.1. North Pacific province $\delta^{13}C$ and $\delta^{15}N$ values

North Pacific biogeochemical marine provinces used in this study were adapted from Longhurst (2007) and are defined by unique hydrographic and biological processes (Fig. 1A). We further characterized these provinces isotopically by compiling mean $\delta^{13}C$ and $\delta^{15}N$ baseline values from the literature for each region. We used isotope data from a combination of particulate organic matter (POM) of the upper 100 m of the water column, primary consumers (e.g. zooplankton) corrected for TL, or organic matter from surface sediment (<100 m depth). Lastly, we used primary producer and primary consumer $\delta^{13}C_{AA}$ and $\delta^{15}N_{AA}$ data for baseline isotope values when available (Supplement 5).

We found significant differences in baseline isotope values of marine provinces for both $\delta^{13}C$ ($F_{5,538}$ = 12.98, $p < 0.001$) and $\delta^{15}N$ ($F_{5,542}$ = 57.48, $p < 0.001$); see Supplement 5 for results of pairwise comparisons among provinces. Overall, North Pacific baseline $\delta^{13}C$ and $\delta^{15}N$ values ranged from −25 to −19‰ and −3.0 to 9.0‰ respectively (Fig. 1B). The North Pacific Subtropical Gyre (NPSG) had the lowest mean $\delta^{15}N$ value (−1.1 ± 1.9‰), and California Cur-

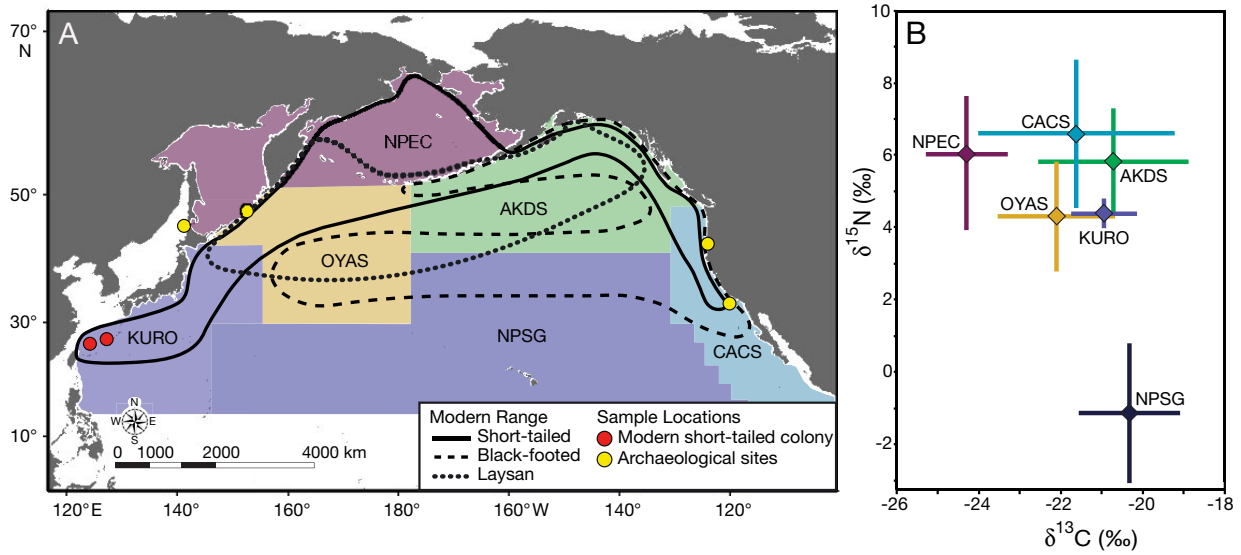

Fig. 1. (A) Modern non-breeding season distributions of North Pacific albatrosses, location of modern short-tailed albatross breeding colonies, and archaeological sites that were sources of the ancient short-tailed albatross analyzed in this study. Modern distributions were estimated from satellite-tracking and ship-based observations (Piatt et al. 2006, Finkelstein et al. 2010, Suryan & Fischer 2010). Note the potential for overlap of short-tailed and black-footed albatross in nearshore habitats in the northeast Pacific from Alaska to California, but black-footed are more common than short-tailed in this region today. Colored regions denote published biogeographical provinces based on geographical variation in hydrographic and biological processes (Longhurst 1998, 2007). NPEC: North Pacific Epicontinental Province (Bering Sea and Sea of Okhotsk); OYAS: Oyashio Current (Western Pacific); KURO: Kuroshio Current; NPSG: North Pacific Subtropical Gyre; AKDS: Alaskan Downwelling System (Gulf of Alaska); CACS: California Current System. (B) Baseline mean $\delta^{13}C$ and $\delta^{15}N$ isotope values of each marine province shown in (A); error bars: ±1 SD. Marine province isotope values were calculated from published and unpublished data (Supplement 5)

rent System (CACS) displayed the highest $\delta^{15}N$ value (6.6 ± 2.1‰). Kuroshio Current (KURO) and Oyashio Current (OYAS) both had intermediate $\delta^{15}N$ values (4–5‰). For $\delta^{13}C$, North Pacific Epicontinental Province (NPEC) had the lowest values (–24.3 ± 1.0‰), in contrast, $\delta^{13}C$ baseline values ranged from –18.5 to –22.0‰ at lower latitudes such as the NPSG and the Alaska Downwelling System (AKDS). KURO had more positive $\delta^{13}C$ values (–20.9 ± 0.8‰) than OYAS (–22.1 ± 1.4‰).

3.2. Albatross bulk tissue $\delta^{13}C$ and $\delta^{15}N$

We found significant differences in bulk bone collagen $\delta^{13}C$ ($F_{6,249}$ = 64.57, p < 0.001) and $\delta^{15}N$ ($F_{6,249}$ = 49.97, p < 0.001) isotope values (Fig. 2) among modern albatross species and ancient short-tailed albatross sourced from the eastern and western North Pacific; see Table 1 for sample sizes, mean isotope values (±SD), and results of pairwise comparisons among species and groups. Briefly, however, bulk $\delta^{13}C$ and $\delta^{15}N$ values for modern albatrosses ranged from about –19 to –14‰ and 14 to 19‰ respectively. Ancient short-tailed albatross generally had higher $\delta^{13}C$ and $\delta^{15}N$ values compared with the modern seabirds: $\delta^{13}C$ and $\delta^{15}N$ values ranged from –17 to –13.0‰ and 15 to 21‰ respectively. There was a greater range (~5‰) in $\delta^{15}N$ values for modern black-footed albatross in comparison with the other 2 (modern) seabird species (~3‰ range) and ancient short-tailed albatross (~3–4‰ range).

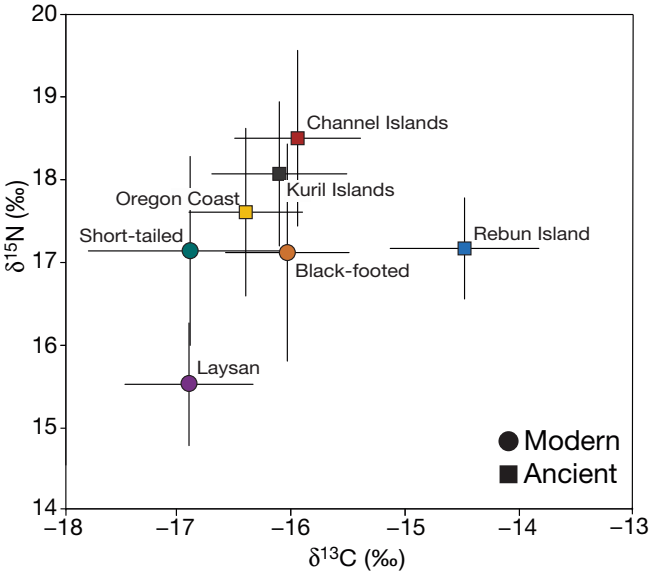

Fig. 2. Bone collagen mean $\delta^{13}C$ and $\delta^{15}N$ values of modern and ancient albatrosses; error bars: ±1 SD. Ancient seabird bones (~1000 yr) were corrected for the Suess Effect for the rate of $\delta^{13}C$ decrease in the atmosphere (see Section 2.2.)

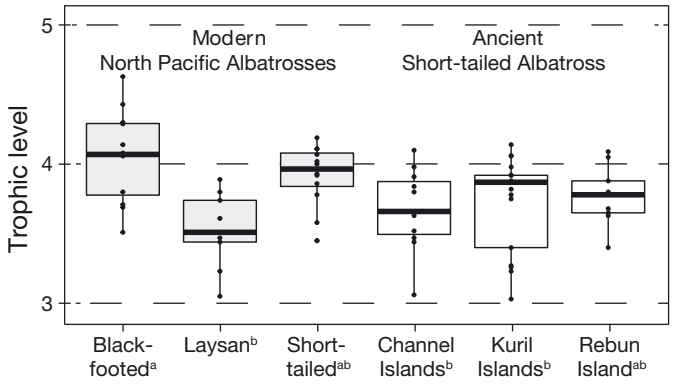

Fig. 3. Trophic level estimates based on amino acid $\delta^{15}N$ data for modern and ancient albatrosses. Black dots are individual data points, box represents the upper and lower quartile, line within box is the median, and whiskers are the maximum and minimum spread of the data. Any data point not connected to a whisker is an outlier. Different superscript letters next to seabird group denote significance

3.3. AA-based estimates of albatross TL

Estimates of trophic level based on TL_{Pro} ranged from 3.5 to 4.1 (Fig. 3), where black-footed had the highest TL and Laysan had the lowest. We found significant differences in TL ($F_{2,75}$ = 4.5, p = 0.001) among albatross species (Table 1); pairwise comparisons showed that black-footed occupied a higher TL than ancient short-tailed from the Channel (p = 0.03) and Kuril Islands (p = 0.02), as well as modern Laysan (p = 0.01) albatross. Modern short-tailed had a higher mean TL (3.9) than their ancient counterparts (3.7–3.8), however, this difference was not significant (Channel Islands p = 0.99; Kuril Islands p = 0.17; Rebun Island p = 0.07).

3.4. AA-derived baseline $\delta^{13}C$ and $\delta^{15}N$ estimates from albatrosses

SEAs based on $\delta^{13}C_{Baseline}$ and $\delta^{15}N_{Baseline}$ data represent the isotopic niche width (units: ‰^{2}) of baseline sources of primary production in foraging habitats used by modern and ancient albatrosses (Fig. 4, Supplement 6). Baseline isotopic niche widths for modern and ancient albatrosses showed similar patterns to the bulk data set (Fig. 2), with a few exceptions. Modern black-footed albatross had the broadest baseline isotopic niche width (5.0‰^{2}), which overlapped with both Laysan and short-tailed, both which had relatively smaller baseline isotopic niche widths (1.5–3.5‰^{2}; Fig. 4A). Laysan had distinctly lower $\delta^{13}C_{Baseline}$ and slightly lower $\delta^{15}N_{Baseline}$ values compared to the other species. Ancient short-tailed albatross had $\delta^{15}N_{Baseline}$ values similar to their mod-

Table 1. Sample $\delta^{13}C$ and $\delta^{15}N$ values of albatross bone collagen for bulk tissue and amino acid isotope analysis (CSIA). Different superscript letters denote significance for bulk tissue $\delta^{13}C$ and $\delta^{15}N$ values, and amino acid $\delta^{13}C$ and $\delta^{15}N$ baseline values, and $\delta^{15}N$-based trophic level estimates. Note there were no significant differences between $\delta^{15}N$ baseline isotope values

	Bulk tissue				Amino acids					Trophic level	$\delta^{15}N_{Baseline}$ (‰)
	n	$\delta^{13}C$ (‰) Mean ± SD	$\delta^{13}C$ (‰) Range	$\delta^{15}N$ (‰) Mean ± SD	$\delta^{15}N$ (‰) Range	n	$\delta^{13}C_{Phe}$ (‰) Mean ± SD	$\delta^{13}C_{Baseline}$ (‰) Mean ± SD	$\delta^{15}N_{Pro}$ (‰) Mean ± SD	$\delta^{15}N_{Phe}$ (‰) Mean ± SD	Mean ± SD	Mean ± SD
Modern											
Black-footed	39	−16.0 ± 0.5^a	−14.3 to −16.8	17.1 ± 1.3^a	19.3 to 14.1	12	−26.9 ± 1.9	−22.4 ± 2.1^{ab}	26.5 ± 2.1	7.5 ± 0.8	4.1 ± 0.3^a	5.7 ± 0.8
Laysan	54	−16.9 ± 0.6^b	−15.4 to −18.2	15.5 ± 0.7^d	16.9 to 13.8	9	−28.4 ± 0.8	−24.0 ± 0.9^a	23.4 ± 1.2	7.1 ± 0.8	3.5 ± 0.3^b	5.4 ± 0.8
Short-tailed	7	−16.9 ± 0.9^b	−16.1 to −18.6	17.1 ± 1.1^{ac}	18.6 to 15.1	13	−26.4 ± 1.1	−21.8 ± 1.2^{bc}	26.3 ± 0.7	8.1 ± 1.1	3.9 ± 0.3^{ab}	6.3 ± 1.1
Ancient short-tailed											
Channel Islands	49	−15.9 ± 0.5^a	−14.8 to −17.3	17.3 ± 0.6^b	20.7 to 16.7	17	−25.1 ± 1.6	−20.1 ± 1.7^{cd}	25.2 ± 1.4	7.9 ± 1.3	3.7 ± 0.3^b	6.5 ± 1.3
Kuril Islands	35	−16.1 ± 0.6^a	−15.0 to −17.0	18.5 ± 1.1^{bc}	20.2 to 16.4	11	−23.6 ± 0.7	−18.7 ± 0.8^d	25.2 ± 1.6	8.2 ± 1.3	3.7 ± 0.3^b	6.4 ± 1.3
Rebun Island	56	−14.7 ± 0.8^c	−13.0 to −16.5	18.1 ± 0.9^a	18.7 to 16.3	9	−23.9 ± 0.8	−19.0 ± 0.9^d	25.6 ± 0.9	8.6 ± 1.2	3.8 ± 0.2^{ab}	6.8 ± 1.2
Oregon Coast	16	−16.4 ± 0.5^{ab}	−14.3 to −16.1	17.6 ± 1.0^{ac}	19.3 to 15.2	–	–	–	–	–	–	–

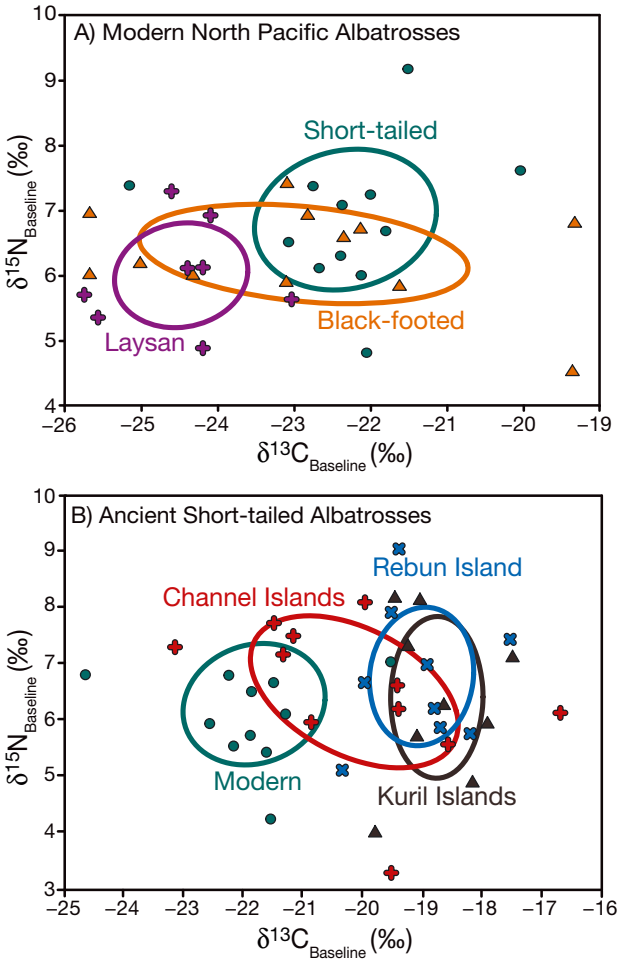

Fig. 4. Baseline production values estimated from amino acid (phenylalanine) $\delta^{13}C$ and $\delta^{15}N$ values of bone collagen of (A) modern albatross and (B) ancient short-tailed albatross. Colored ellipses represent the standard bivariate ellipse areas for each of the groups. See Section 2.3. for how baseline isotope values were calculated

ern congeners but in general had higher $\delta^{13}C_{Baseline}$ values (Fig. 4B). Ancient short-tailed albatross from the Channel Islands in the eastern Pacific had the largest baseline isotopic niche breadth (6.5‰^{2}; Fig. 4B). Ancient short-tailed albatross from Rebun Island and the Kuril Islands in the western Pacific had overlapping baseline isotopic niches (3.5‰^{2}), which contrasts with the patterns in the bulk tissue data set (Fig. 2) where ancient short-tailed albatross from the Channel and Kuril Islands had overlapping isotope values and specimens from Rebun Island had distinctly higher $\delta^{13}C$ values. Overall, both the bulk tissue and AA baseline data indicate that ancient short-tailed albatross had higher $\delta^{13}C_{Baseline}$ and $\delta^{15}N_{Baseline}$ values than their modern counterparts and other North Pacific albatross species (Table 1).

3.5. Foraging distribution

The bulk tissue data corrected for TL based on AA $\delta^{15}N$ results (TL_{Pro}) was used in the SIAR mixing model because it was a much larger data set, therefore enhancing statistical resolution (see Supplement 7 at www.int-res.com/articles/suppl/m610p001_supp7.xlsx for detailed isotope data). Based on model output, all individual albatrosses fell within the range of baseline values for the marine provinces (Fig. 5A) and used multiple marine provinces to forage (Fig. 5B). Modern black-footed albatross baseline isotope signatures predominately overlapped in NPEC (40%) followed by NPSG (25%) and then AKDS (~15%). Modern Laysan albatross overlapped in the more northwestern provinces with about equal distribution in NPEC (30%), OYAS (~20%), and KURO (~20%). Obtaining samples of modern short-tailed albatross was very difficult and thus our sample size is relatively small (n = 7), however, mixing models indicate highest overlap in NPEC (~40%), and ~5–20% for the remaining marine provinces (e.g. AKDS and OYAS). Ancient short-tailed albatross predominately overlapped with marine provinces in the eastern Pacific. Ancient short-tailed albatross from the Channel Islands had the highest overlap with the CACS (50%) and AKDS (30%) provinces. Ancient short-tailed from the Kuril Islands had equal overlap in CACS (40%) and AKDS (40%), and ancient specimens from Rebun Island overlapped most with AKDS (70%) followed by CACS (20%).

4. DISCUSSION

Our bulk tissue and compound-specific isotopic approach enabled us to generate a broad population-level understanding of both modern and historical North Pacific albatross ecology. The overall patterns in both the bulk tissue data (Fig. 2) and AA-based estimates of isotopic baseline (Fig. 4) were in general agreement, suggesting that the primary driver for observed offsets in bulk tissue isotope values among species and/or ancient versus modern populations is geographical differences in foraging regions, with the secondary driver likely being variation in diet composition (e.g. TL). In the following subsections, we first discuss the underlying mechanisms of marine province isoscape patterns. We then compare TL estimates in the context of diet data for North Pacific albatrosses based on genetic techniques, and validate our isotopic approach by comparing it to known movement patterns of the 3 modern North Pacific

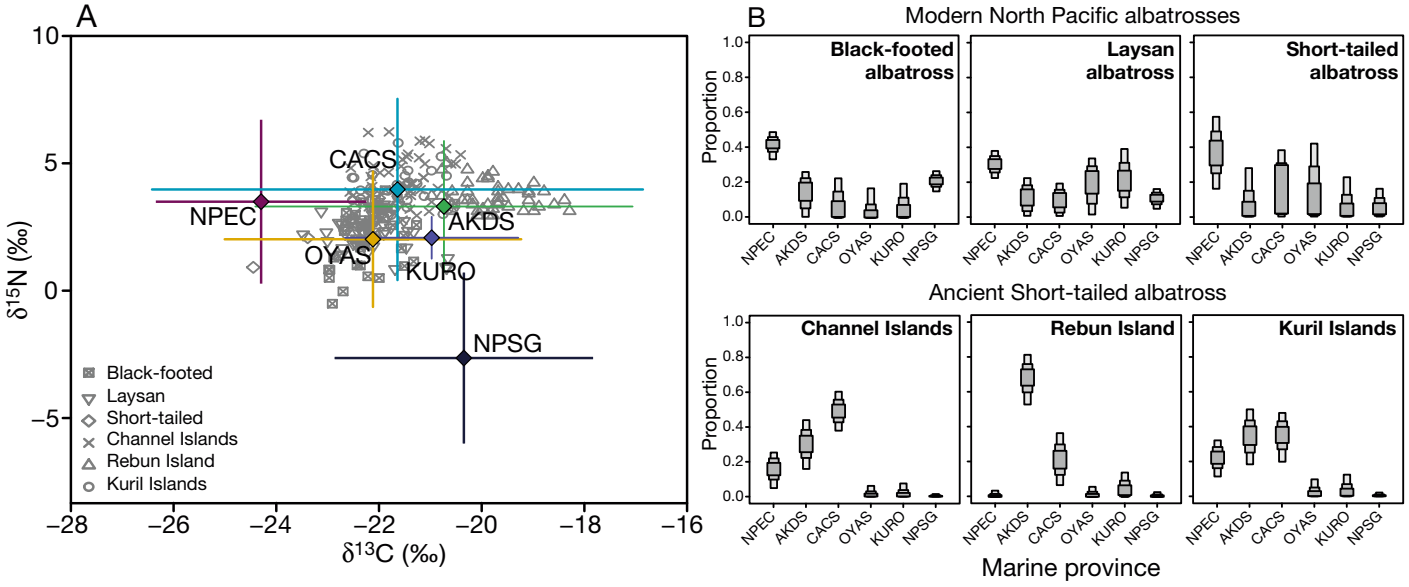

Fig. 5. (A) Biplot of mean baseline $\delta^{13}C$ and $\delta^{15}N$ values of North Pacific marine province values (see Fig. 1B) and modern and ancient albatrosses: black-footed, Laysan, short-tailed, Channel Island, Rebun Island, Kuril Islands; error bars: ±1 SD. We trophic-corrected $\delta^{15}N$ values by adding 3.1‰ per trophic step, where trophic level estimates were determined for each species using amino acid nitrogen isotope analysis (see Fig. 3). (B) Mixing model results as proportion of foraging habitat for modern albatross and ancient short-tailed albatross; boxes represent ±50, ±75, and ±95% credibility intervals. See Fig. 1 for biogeographical province abbreviations

albatross species based on satellite telemetry. Finally, we interpret the historical movement and foraging behavior of short-tailed albatross from 3 archaeological sites, 2 in the western and 1 in the eastern North Pacific, in the context of what is known about the ecology of the rapidly growing modern short-tailed albatross population.

4.1. North Pacific oceanographic province isoscapes

Low $\delta^{15}N$ values (–1.1 ± 1.9‰) in the NPSG are commonly attributed to N_2-fixation by diazatrophic cyanobacteria (Capone et al. 1997). Conversely, the CACS high $\delta^{15}N$ values (6.6 ± 2.1‰) are due to the northward flowing California undercurrent, which carries denitrified waters with characteristically high nitrate (NO_3) $\delta^{15}N$ values from the eastern tropical North Pacific (Altabet et al. 1999, Voss et al. 2001, Vokhshoori & McCarthy 2014). The KURO and OYAS both have intermediate $\delta^{15}N$ values (4–5‰), indicative of regions in which nitrogen could be sourced from a combination of upwelled NO_3 and/or N_2-fixation (Yamazaki et al. 2011). For $\delta^{13}C$, the most northern marine province in our study, the NPEC, had the lowest values (–24.3 ± 1.0‰). Primary producers in high-latitude waters typically have lower $\delta^{13}C$ values relative to those in temperate and tropical latitudes, primarily because of higher dissolution of CO_2 into colder seawater that increases the carbon isotope fractionation between phytoplankton cells and CO_2 ($\delta^{13}C$), lower phytoplankton growth rates, and phytoplankton community dynamics typically characterized by seasonal blooms of large phytoplankton cells (Rau et al. 1982, Goericke & Fry 1994). In contrast, $\delta^{13}C$ baseline values ranged from –18.5 to –22.0‰ at lower latitudes such as the NPSG, which is likely caused by a combination of lower [CO_2] in warmer waters and correspondingly lower $\delta^{13}C$, higher phytoplankton growth rates, nutrient limitation, and fractionation effects associated with small phytoplankton cell size (Bidigare et al. 1997, Popp et al. 1998). The AKDS also had higher $\delta^{13}C$ values, likely linked to enhanced productivity and larger cells (Pomerleau et al. 2014, Hertz et al. 2016). While downwelling systems are typically associated with low productivity, the AKDS is highly productive due to eddies and advection that delivers resuspended nutrients to the continental shelf (Stabeno et al. 2004). The KURO had more positive $\delta^{13}C$ values (–20.9 ± 0.8‰) than OYAS (–22.1 ± 1.4‰). The KURO is a fast, warm water western boundary current that transports equatorial waters northward. The OYAS, also a western boundary current, transports cold water from the subarctic southward and therefore has lower $\delta^{13}C$ isotope values than the KURO.

4.2. Trophic level

The TL_{Pro} values we measured for both modern and ancient North Pacific albatross (3.1 to 4.6; Fig. 3) are consistent with the few studies that report TLs for the Diomedeidae family (3.5 to 5.3; Sydeman et al. 1997, Cherel et al. 2010). We therefore believe our TL estimates that utilize proline as the primary trophic AA are reasonable. Albatross are opportunistic foragers that prey on and/or scavenge a combination of intermediate and higher TL organisms such as squid, flying fish, or even marine mammal carrion, as well as small lanternfishes, crustaceans, and cnidarians near the base of the food chain (Harrison et al. 1983, Walker et al. 2015, McInnes et al. 2017, Conners et al. 2018). Modern black-footed albatross clearly forage at a higher TL than modern Laysan and short-tailed albatross, a pattern consistent with previous observations (Fig. 3; Harrison et al. 1983, Gould et al. 1997, Walker et al. 2015, Conners et al. 2018). Another intriguing pattern in our results is that modern short-tailed albatross occupy a slightly but not significantly higher TL than all 3 ancient short-tailed populations, which suggests that the trophic ecology of short-tailed albatross may have shifted in response to increasing human disturbance of their open-ocean pelagic habitat. We hypothesize that this could be a consequence of the modern seabird's interaction with commercial fisheries, where high TL prey in the form of bycatch, processor discards (offal), and baits (Pacific saury *Cololabis saira* and Argentine shortfin squid *Illex argentinus*) used in long-line fisheries in the North Pacific (Walker et al. 2015) are spatially concentrated by such open-ocean fishing techniques, making it easier for albatrosses (and other seabird species) to opportunistically scavenge this novel resource. Both black-footed and Laysan albatrosses routinely exploit such resources (Fischer et al. 2009), and the primary threat to short-tailed albatross recovery is entanglement in longlining fishing gear (Suryan et al. 2007); see Supplement 3 for further discussion of TL.

4.3. Foraging habitats

The marine province designations derived from our isotope mixing model agree with satellite and observation-based studies of North Pacific albatross movement patterns. Black-footed and Laysan albatross share nesting grounds in the central Pacific (Hyrenbach et al. 2002) and overlap to a large degree during the breeding season (December to April), but these species use different regions of the North Pacific during the non-breeding season from June to October (Fig. 1; Suryan & Fischer 2010). Overall, these patterns result in these 2 species largely exploiting different regions over multi-year timescales (Fig. 1). For this study, black-footed and Laysan albatross included specimens collected from Hawaiian and northwestern Alaskan fisheries, whereas short-tailed albatross included bycaught specimens from the Pacific cod *Gadus macrocephalus* fishery in the Bering Sea and Aleutian Islands and one beach-cast specimen from Morro Bay, CA. Our results show that black-footed and Laysan albatross have some isotopic overlap with the subtropical gyre region (10–15%; Fig. 5B), which might reflect time spent foraging in this region during the breeding season (Hyrenbach et al. 2002). Throughout the year, but more apparent outside of the breeding season, Laysan albatross spend the greatest amount of time in oceanic pelagic waters away from the continental shelf (Fischer et al. 2009, Suryan & Fischer 2010), and in the Kuroshio Extension southwest of Hawaii (Fisher & Fisher 1972, Fernández et al. 2001). This movement pattern is likely reflected in the relatively low $\delta^{13}C_{Baseline}$ values for Laysan in comparison to the other albatross species (Fig. 4A; Fry & Wainright 1991, Hemminga & Mateo 1996), while mixing model results show the highest degree of overlap of Laysan to provinces OYAS and KURO that most closely matched the Kuroshio Extension (Fig. 5B). In contrast, the relatively high $\delta^{13}C_{Baseline}$ values we measured for modern short-tailed and black-footed albatrosses confirm that these species spend more time foraging in neritic waters near the continental shelf-slope break. These 2 albatross species typically visit steep bathymetric features such as continental shelf and slope gradients along the Aleutian Island chain and Alaskan current, with short-tailed albatross ranging farther north and black-footed ranging more southeast (Suryan et al. 2006, Kuletz et al. 2014). Our mixing model results therefore correctly assigned black-footed albatross a foraging range in Aleutian Island chain (NPEC) and Gulf of Alaska (AKDS) provinces, and short-tailed baseline isotope signatures overlapped most with NPEC.

The baseline isotopic niche widths (Fig. 4) show that modern black-footed albatross have the broadest foraging range of all the North Pacific species, while Laysan albatross have the narrowest range. This conclusion is supported by satellite telemetry data showing that black-footed albatross in the central North Pacific will fly to shelf-slope breaks along the Aleutian Islands, Gulf of Alaska, and California

Current (Kappes et al. 2010, Suryan & Fischer 2010), while Laysan albatross from the same nesting site typically concentrate within the oceanic habitats in the North Pacific Transition Zone to forage (Hyrenbach et al. 2002, Kappes et al. 2010). The broad baseline isotopic niche width of black-footed albatross may be associated with a range expansion in the last century (T. Dunlap 1988) in response to the historical population collapse of short-tailed albatross (Yesner 1976). Overall, our mixing model results for modern North Pacific albatrosses (Figs. 4 & 5) strongly match published satellite-tracking data (e.g. Kappes et al. 2010, Suryan & Fischer 2010), confirming that this approach is useful for assessing the movement patterns of historical and ancient seabird populations.

Bulk bone collagen tissue and AA data for ancient short-tailed albatross sourced from archaeological sites indicates that they occupied a distinct isotopic niche from their modern counterparts (Figs. 2 & 4B). Specimens from archaeological sites on the Kuril Islands (Russia) and Rebun Island off northern Japan overlap almost entirely in $\delta^{13}C_{Baseline}$ and $\delta^{15}N_{Baseline}$ space, while ancient samples from the Channel Islands have a very large baseline isotopic niche width relative to both modern and other ancient short-tailed albatross. All 3 ancient short-tailed albatross groups had relatively high $\delta^{13}C_{Baseline}$ values, suggesting that they foraged in more nearshore waters and possibly at lower latitudes than the modern population (Rau et al. 1982). Historical sightings of short-tailed albatross support this conclusion, reporting them as abundant in shallow waters of coastal North America, especially off Alaska (Murie 1959). Moreover, short-tailed albatross are thought to have come so close to shore that native people on Kodiak Island sometimes hunted them from kayaks (Hasegawa & DeGange 1982).

Our isotope mixing model results indicate that ancient short-tailed albatross populations have the largest degree of overlap with AKDS and CACS (Fig. 4B). However, while zooarchaeological records and isotopic reconstructions can help characterize former foraging habitats, distinguishing between former breeding grounds and areas of high abundance with zooarchaeological data alone is difficult without evidence of eggshells or bones of pre-fledged chicks. For example, in the Aleutians, particularly Umnak Island and Four Mountains, Kotzube (1826) recounts that native Aleuts exploited short-tailed albatross nests for birds and eggs. Further, other explorers like Dall (1872) believed short-tailed albatross bred in the Aleutian Islands, having seen mutilated carcasses of very young birds. Zooarchaeological remains from the family Diomedeidae (especially short-tailed albatross) are prevalent in sites on the Japanese Islands (Eda & Higuchi 2004), Aleutian Island Chain (Yesner 1976), and North America (Howard & Dodson 1933, Friedman 1934, Murie 1959). For example, short-tailed albatross are frequently one of the most abundant seabird species present in archaeological sites on the Channel Islands off southern California. However, none of these sites contained the remains of fledgling albatross, so it is still uncertain whether short-tailed albatross had nesting grounds in the northeastern Pacific. By analyzing ancient mitochondrial DNA (aDNA) extracted from archaeological samples excavated in southern Japan, Eda et al. (2012) found that short-tailed albatross grouped into 2 distinct populations whose level of genetic divergence exceeded that between sister species of other modern albatross populations. Our results indicate that ancient Channel Island seabirds had a different isotopic niche from the other 2 ancient sites (Fig. 4B), supporting the idea that there were 2 distinct populations of short-tailed albatross. Future work examining aDNA of ancient short-tailed remains from archaeological sites in the Aleutian and Channel Islands could provide a full phylogenetic context for understanding the recent demography of these sub-groups.

4.4. Conclusions

Our results demonstrate that both bulk tissue and AA isotope data are informative for understanding past and present albatross foraging and movement ecology. Our bulk tissue results provided larger sample size to compare our different albatross groupings, while our CSIA data set allowed us to estimate TL and baseline isotope values. We found that ancient short-tailed albatross populations had more positive $\delta^{13}C_{Baseline}$ and $\delta^{15}N_{Baseline}$ values, indicating more use of the California Current and Gulf of Alaska than their modern counterparts. We hypothesize that this is because ancient populations foraged in nearshore habitats at lower latitudes in the eastern North Pacific than they do today. Whether the Aleutian and/or Channel Islands were former nesting grounds still remains uncertain; future work combining our isotopic approach with the analysis of ancient mtDNA could potentially answer this question. North Pacific albatross migratory patterns have shifted in recent decades in response to environmental changes (Kuletz et al. 2014), and while extant populations recover from historic over-exploitation and continue to grow at near capacity (Deguchi et al. 2012), more shifts in

distribution and foraging habitats may occur. For example, Laysan albatross has the largest and most stable extant population of the 3 Diomediedae species endemic to the North Pacific and recently underwent a ~4000 km breeding range expansion to Guadalupe Island off the coast of Mexico where they had not been previously documented (E. Dunlap 1988). Overall, our results indicate a more complex population structure for ancient short-tailed albatross populations in comparison to their modern counterparts, which provides insight into how this species may behave as its population recovers former foraging and perhaps breeding territory. Such data sets highlight the importance of understanding the ecology of species that was truncated by historical human overexploitation and are now living in relict populations.

Acknowledgements. We thank the Smithsonian, Burke Museum of Natural History, Natural History Museum of Los Angeles County, Oregon Museum of Natural and Cultural History, and Santa Barbara Museum of Natural History that provided albatross specimens analyzed in this study. We are grateful to the National Marine Fisheries Service, Alaska Fisheries Science Center, Pacific Islands Regional Office - Fisheries Observer Program staff and observers, the vessels and crew of the fisheries that supported the observers, and Shannon Fitzgerald and Hannah Nevins for facilitating sampling of bycatch specimens. We are also indebted to Viorel Atudorei and Laura Burkemper at the UNM Center for Stable Isotopes, as well as Stephanie Christiansen, Dkye Andresean and Elizabeth Gier at the UC Santa Cruz Stable Isotope Laboratory for help with amino acid isotope analysis, and Calli Hamlin for bulk tissue preparation and isotope analysis.

LITERATURE CITED

Altabet MA, Pilskaln C, Thunell R, Pride C, Sigman D (1999) The nitrogen isotope biogeochemistry of sinking particles from the margin of the eastern North Pacific. Deep Sea Res I 46:655–679

Arata JA, Sievert PR, Naughton MB (2009) Status assessment of Laysan and black-footed albatrosses, North Pacific Ocean, 1923–2005. US Geol Surv Sci Investig Rep 2009:5131

Aurioles D, Koch PL, LeBoeuf BJ (2006) Differences in foraging location of Mexican and California elephant seals: evidence from stable isotopes in pups. Mar Mamm Sci 22:326–338

Bidigare RR, Fluegge A, Freeman KH, Hanson KL and others (1997) Consistent fractionation of ^{13}C in nature and in the laboratory: growth-rate effects in some haptophyte algae. Global Biogeochem Cycles 11:279–292

Burton RK, Snodgrass JJ, Gifford-Gonzalez D, Guilderson T, Brown T, Koch P (2001) Holocene changes in the ecology of northern fur seals: insights from stable isotopes and archaeofauna. Oecologia 128:107–115

Capone DG, Zehr J, Paerl H, Bergman B, Carpenter EJ (1997) *Trichodesmium*: a globally significant marine cyanobacterium. Science 276:1221–1229

Carlisle AB, Kim SL, Semmens BX, Madigan DJ and others (2012) Using stable isotope analysis to understand migration and trophic ecology of northeastern Pacific white sharks (*Carcharodon carcharias*). PLOS ONE 7:e30492

Cherel Y, Fontaine C, Richard P, Labat J (2010) Isotopic niches and trophic levels of myctophid fishes and their predators in the Southern Ocean. Limnol Oceanogr 55: 324–332

Chikaraishi Y, Ogawa NO, Kashiyama Y, Takano Y and others (2009) Determination of aquatic food-web structure based on compound-specific nitrogen isotopic composition of amino acids. Limnol Oceanogr Methods 7: 740–750

Chikaraishi Y, Steffan SA, Ogawa NO, Ishikawa N, Sasaki Y, Tsuchiya M, Ohkouchi N (2014) High-resolution food webs based on nitrogen isotopic composition of amino acids. Ecol Evol 4:2423–2449

Conners MG, Goetsch C, Budge SM, Walker WA, Mitani Y, Costa DP, Shaffer SA (2018) Fisheries exploitation by albatross quantified with lipid analysis. Front Mar Sci 5: 113

Dall WH (1872) Notes on prehistoric remains in the Aleutian Islands. Proc Calif Acad Sci 5:275–279

Deguchi T, Jacobs J, Harada T, Perriman L and others (2012) Translocation and hand-rearing techniques for establishing a colony of threatened albatross. Bird Conserv Int 22:66–81

Deguchi T, Sato F, Eda M, Izumi H, Suzuki H, Suryan RM (2017) Translocation and hand-rearing result in short-tailed albatrosses returning to breed in the Ogasawara Islands 80 years after extirpation. Anim Conserv 20: 341–349

DeNiro MJ, Epstein S (1978) Influence of diet on the distribution of carbon isotopes in animals. Geochim Cosmochim Acta 42:495–506

Dunlap E (1988) Laysan albatross nesting on Guadalupe Island, Mexico. Am Birds 42:180–181

Dunlap T (1988) Saving America's wildlife. Princeton University Press, Princeton, NJ

Eda M, Higuchi M (2004) Distribution of albatross remains in the far east regions during the Holocene, based on zooarchaeological remains. Zool Sci 21:771–783

Eda M, Koike H, Kuro-o M, Mihara S, Hasegawa H, Higuchi H (2012) Inferring the ancient population structure of the vulnerable albatross *Phoebastria albatrus*, combining ancient DNA, stable isotope, and morphometric analyses of archaeological samples. Conserv Genet 13:143–151

Erlandson JM, Rick TC, Braje TJ, Casperson M and others (2011) Paleoindian seafaring, maritime technologies, and coastal foraging on California's Channel Islands. Science 331:1181–1185

Fernández P, Anderson DJ, Sievert PR, Huyvaert KP (2001) Foraging destinations of three low-latitude albatross (*Phoebastria*) species. J Zool (Lond) 254:391–404

Finkelstein M, Wolf S, Goldman M, Sievert P, Balogh G, Hasegawa H, Doak DF (2010) The anatomy of a disaster: volcanoes, behavior, and life history of the short-tailed albatross (*Phoebastria albatrus*). Biol Conserv 143:321–331

Fischer KN, Suryan RM, Roby DD, Balogh GR (2009) Post-breeding season distribution of black-footed and Laysan albatrosses satellite-tagged in Alaska: inter-specific differences in spatial overlap with North Pacific fisheries. Biol Conserv 142:751–760

Fisher HI, Fisher JR (1972) The oceanic distribution of the Laysan albatrosses, *Diomedea immutabilis.* Wilson Bull 84:7–27

Francey RJ, Allison CE, Etheridge DM, Trudinger CM and others (1999) A 1000-year high precision record of $\delta^{13}C$ in atmospheric CO_2. Tellus B Chem Phys Meterol 51: 170–193

Friedman H (1934) Bird bones from Eskimo ruins on St. Lawrence Island, Bering Sea. J Wash Acad Sci 24:83–96

Fry B, Wainright SC (1991) Diatom sources of ^{13}C-rich carbon in marine food webs. Mar Ecol Prog Ser 76:149–157

Goericke R, Fry B (1994) Variations of marine plankton $\delta^{13}C$ with latitude, temperature, and dissolved CO_2 in the world ocean. Global Biogeochem Cycles 8:85–90

Gould P, Ostrom P, Walker W (1997) Trophic relationships of albatrosses associated with squid and large-mesh drift-net fisheries in the North Pacific Ocean. Can J Zool 75: 549–562

Graham BS, Koch PL, Newsome SD, McMahon KW, Aurioles D (2010) Using isoscapes to trace the movements and foraging behavior of top predators in oceanic ecosystems. In: West JB, Bowen GJ, Dawson TE, Tu KP (eds) Isoscapes. Springer, Houten, p 299–318

Hare EP, Fogel ML, Stafford TW, Mitchell AD, Hoering TC (1991) The isotopic composition of carbon and nitrogen in individual amino acids isolated from modern and fossil proteins. J Archaeol Sci 18:277–292

Harrison CS, Hida TS, Seki M (1983) Hawaiian seabird feeding ecology. Wildl Monogr 85:1–71

Hasegawa H, DeGange AR (1982) The short-tailed albatross, *Diomedea albatrus*, its status, distribution and natural history. Am Birds 36:806–814

Hemminga MA, Mateo MA (1996) Stable carbon isotopes in seagrasses: variability in ratios and use in ecological studies. Mar Ecol Prog Ser 140:285–298

Hertz E, Trudel M, Tucker S, Beacham TD, Parken C, Mackas D, Mazumder A (2016) Influences of ocean conditions and feeding ecology on the survival of juvenile chinook salmon (*Oncorhynchus tshawytscha*). Fish Oceanogr 25:407–419

Hobson KA, Clark RG (1992) Assessing avian diets using stable isotopes II: Factors influencing diet-tissue fractionation. Condor 94:189–197

Howard H, Dodson L (1933) Bird remains from an Indian shell-mound near Point Mugu, California. Condor 35:235

Howland MR, Corr LT, Young SMM, Jones V and others (2003) Expression of the dietary isotope signal in the compound-specific $\delta^{13}C$ values of pig bone lipids and amino acids. Int J Osteoarchaeol 13:54–65

Hyrenbach KD, Fernández P, Anderson DJ (2002) Oceanographic habitats of two sympatric North Pacific albatrosses during the breeding season. Mar Ecol Prog Ser 233:283–301

Jackson JB, Kirby MX, Berger WH, Bjorndal KA, Botsford WA (2001) Historical overfishing and the recent collapse of coastal ecosystems. Science 293:629–638

Jackson AL, Inger R, Parnell AC, Bearhop S (2011) Comparing isotopic niche widths among and within communities: SIBER—stable isotope Bayesian ellipses in R. J Anim Ecol 80:595–602

Kappes MA, Shaffer SA, Tremblay Y, Foley DG and others (2010) Hawaiian albatrosses track interannual variability of marine habitats in the North Pacific. Prog Oceanogr 86:246–260

Kotzube OV (1826) A voyage of discovery in to the South Sea and Bering's Straits. Reissued 1967. Da Capo Press, New York, NY

Kuletz KJ, Renner M, Labunski EA, Hunt GL (2014) Changes in the distribution and abundance of albatrosses in the eastern Bering Sea: 1975-2010. Deep Sea Res II 109: 282–292

Larsen T, Ventura M, Andersen N, O'Brien DM, Piatkowski U, McCarthy MD (2013) Tracing carbon sources through aquatic and terrestrial food webs using amino acid stable isotope fingerprinting. PLOS ONE 8e73441

Laws EA, Popp BN, Bidigare RP, Kennicutt MC, Macko SA (1995) Dependence of phytoplankton carbon isotopic composition on growth rate and $[CO_2]_{aq}$: theoretical consideration and experimental results. Geochim Cosmochim Acta 59:1131–1138

Longhurst A (1998) Ecological geography of the sea. Academic Press, London

Longhurst A (2007) Ecological geography of the sea, 2nd edn. Academic Press, Burlington, MA

Lorrain A, Graham BS, Popp BN, Allain V and others (2015) Nitrogen isotopic baselines and implications for estimating foraging habitat and trophic position of yellowfin tuna in the Indian and Pacific Oceans. Deep Sea Res II 113:188–198

Lotze HK, Worm B (2009) Historical baselines for large marine animals. Trends Ecol Evol 24:254–262

Madigan DJ, Baumann Z, Carlisle AB, Hoen DK and others (2014) Reconstructing trans-oceanic migration patterns of Pacific bluefin tuna using a chemical tracer toolbox. Ecology 95:1674–1683

McClelland JW, Montoya JP (2002) Trophic relationships and the nitrogen isotopic composition of amino acids. Ecology 83:2173–2180

McInnes JC, Alderman R, Raymond B, Lea MA, Deagle B, Phillips RA (2017) High occurrence of jellyfish predation by black-browed and Campbell albatross identified by DNA metabarcoding. Mol Ecol 26:4831–4845

McMahon KW, McCarthy MD (2016) Embracing variability in amino acid $\delta^{15}N$ fractionation: mechanisms, implications, and applications for trophic ecology. Ecosphere 7: e01511

McMahon KW, Ling Hamady L, Thorrold SR (2013) A review of ecogeochemistry approaches to estimating movements of marine animals. Limnol Oceanogr 58:697–714

McMahon KW, McCarthy MD, Sherwood OA, Larsen T, Guilderson TP (2015) Millennial-scale plankton regime shifts in the subtropical North Pacific Ocean. Science 350:1530–1533

Murie OJ (1959) Fauna of the Aleutian Islands and Alaska Peninsula. US Government Printing Office, Washington, DC

Newsome SD, Etnier MA, Gifford-Gonzalez D, Phillips DL and others (2007) The shifting baseline of northern fur seal ecology in the northeast Pacific Ocean. Proc Natl Acad Sci USA 104:9709–9714

O'Connell TC (2017) 'Trophic' and 'source' amino acids in trophic estimation: a likely metabolic explanation. Oecologia 184:317–326

Olson SL, Hearty PJ (2003) Extirpation of a breeding colony of short-tailed albatross (*Phoebastria albatrus*) on Bermuda by Pleistocene sea-level rise. Proc Natl Acad Sci USA 100:12825–12829

Parnell AC, Inger R, Bearhop S, Jackson AL (2010) Source partitioning using stable isotopes: coping with too much variation. PLOS ONE 5:e9672

Piatt JF, Wetzel J, Bell K, DeGange AR and others (2006) Predictable hotspots and foraging habitat of the endangered short-tailed albatross (*Phoebastria albatrus*) in the North Pacific: implications for conservation. Deep Sea Res II 53:387-398

Pomerleau C, Nelson RJ, Hunt BPV, Sastri AK, Williams WJ (2014) Spatial patterns in zooplankton communities and stable isotope ratios ($\delta^{13}C$ and $\delta^{15}N$) in relation to oceanographic conditions in the sub-Arctic Pacific and western Arctic regions during the summer of 2008. J Plankton Res 36:757–775

Popp BN, Laws EA, Bidigare RR, Dore JE, Hanson KL, Wakeman SG (1998) Effect of phytoplankton cell geometry on carbon isotopic fractionation. Geochim Cosmochim Acta 62:69–77

Popp BN, Graham BS, Olson RJ, Hannides CCS and others (2007) Insight into the trophic ecology of yellowfin tuna, *Thunnus albacares*, from compound-specific nitrogen isotope analysis of proteinaceous amino acids. In: Dawson T, Seigwolf R (eds) Isotopes as tracers in ecological change. Elsevier, New York, NY, p 173–190

Porcasi JF (1999) Prehistoric exploitation of albatross on the Southern California Channel Islands. J Calif Gt Basin Anthropol 21:60–68

Quay PD, Tilbrook B, Wong CS (1992) Oceanic uptake of fossil fuel CO_2: Carbon-13 evidence. Science 256:74–79

Rau GH, Sweeney RE, Kaplan IR (1982) Plankton ^{13}C:^{12}C ratio changes with latitude: differences between northern and southern oceans. Deep Sea Res I 29:1035–1039

Rau GH, Takahashi T, Desmarais DJ (1989) Latitudinal variations in plankton $\delta^{13}C$: implications for CO_2 and productivity in past oceans. Nature 341:516–518

Sigman DM, Kash KL, Casciotti KL (2009) Ocean process tracers: nitrogen isotopes in the ocean. Encyclopedia of ocean science, 2nd edn. Elsevier, Amsterdam

Silfer JA, Engel MH, Macko SA, Jumeau EJ (1991) Stable carbon isotope analysis of amino acid enantiomers by conventional isotope ratio mass spectrometry and combined gas chromatography/isotope ratio mass spectrometry. Anal Chem 63:370–374

Stabeno PJ, Bond NA, Hermann AJ, Kachel NB, Mordy CW, Overland JE (2004) Meteorology and oceanography of the northern Gulf of Alaska. Cont Shelf Res 24:859–897

Suryan RM, Fischer KN (2010) Stable isotope analysis and satellite tracking reveal interspecific resource partitioning of nonbreeding albatrosses off Alaska. Can J Zool 88: 299–305

Suryan RM, Sato F, Balogh GR, Hyrenbach KD, Sievert PR, Ozaki K (2006) Foraging destinations and marine habitat use of short-tailed albatrosses: a multi-scale approach using first-passage time analysis. Deep Sea Res II 53: 370–386

Suryan RM, Dietrich KS, Melvin EF, Balogh GR, Sato F, Ozaki K (2007) Migratory routes of short-tailed albatrosses: use of exclusive economic zone of North Pacific Rim countries and spatial overlap with commercial fisheries in Alaska. Biol Conserv 137:450–460

Swetnam TW, Allen CD, Betancourt JL (1999) Applied historical ecology: using the past to manage for the future. Ecol Appl 9:1189–1206

Sydeman WJ, Hobson KA, Pyle P, McLaren EB (1997) Trophic relationships among seabirds in central California: combined stable isotope and conventional dietary approach. Condor 99:327–336

Turner Tomaszewicz CN, Seminoff JA, Peckham HS, Avens L, Kurle CM (2017) Intrapopulation variability in the timing of ontogenetic habitat shifts in sea turtles revealed using ^{15}N values from bone growth rings. J Anim Ecol 86:694–704

USFWS (US Fish and Wildlife Service) (2008) Birds of conservation concern. United States Department of Interior, Fish and Wildlife Service, Division of Migratory Bird Management, Arlington, VA. https://www.fws.gov/migratorybirds/pdf/grants/birdsofconservationconcern2008.pdf/

Vanderklift MA, Ponsard S (2003) Sources of variation in consumer-diet ^{15}N enrichment: a meta-analysis. Oecologia 136:169–182

Vokhshoori NL, McCarthy MD (2014) Compound-specific ^{15}N amino acid measurements in littoral mussels in the California upwelling ecosystem: a new approach to generating baseline $\delta^{15}N$ isoscapes for coastal ecosystems. PLOS ONE 9:e98087

Vokhshoori NL, Larsen T, McCarthy MD (2014) $\delta^{13}C$ of amino acids in littoral mussels: a new approach to constructing isoscapes of primary production in a coastal upwelling system. Mar Ecol Prog Ser 504:59–72

Voss M, Dippner JW, Montoya JP (2001) Nitrogen isotope patterns in the oxygen-deficient waters of the eastern tropical North Pacific Ocean. Deep Sea Res I 48: 1905–1921

Walker WA, Fitzgerald SM, Collins PW (2015) Stomach contents of seven short-tailed albatrosses *Phoebastria albatrus* in the Eastern North Pacific and Bering Sea. Mar Ornithol 43:169–172

Wiley AE, Ostrom PH, Welch AJ, Fleischer RC and others (2013) Millenial-scale isotope records from a wide-ranging predator show evidence of recent human impact to oceanic food webs. Proc Natl Acad Sci USA 110: 8972–8977

Yamazaki A, Watanabe T, Tsunogai U (2011) Nitrogen isotopes of organic nitrogen in reef coral skeletons as a proxy of tropical nutrient dynamics. Geophys Res Lett 38: L19605

Yesner DR (1976) Aleutian Island albatrosses: a population history. Auk 93:263–280

Editorial responsibility: Stephen Wing, Dunedin, New Zealand

Submitted: August 20, 2018; Accepted: December 3, 2018
Proofs received from author(s): January 8, 2019